Selection mechanism and area distribution in two-dimensional cellular structures

Daniel Segel and David Mukamel
Department of Nuclear Physics, Weizmann Institute of Science, Rehovot 76100, Israel

Oleg Krichevsky and Joel Stavans
Department of Electronics, Weizmann Institute of Science, Rehovot 76100, Israel

(Received 9 September 1992)

Evolving random cellular structures are observed to reach a universal scaling regime. A mean-field approach to finding fixed-point distributions in cell-side number is extended to distributions for the average area of cells with a given number of sides. This approach leads to simplified equations that can be analyzed analytically and numerically. The theory's results are compared to experimental results on dynamics and distributions in soap froths and good agreement is achieved.

PACS number(s): 02.50.+s, 82.70.Rr

I. INTRODUCTION

Many examples of random cellular structures, in which cells have random areas and numbers of sides, exist in nature [1]. These include polycrystals [2–4], magnetic bubbles in garnets [5–8], foams, and soap froths [9,10]. These systems exhibit structures which coarsen continually with time without reaching thermal equilibrium. Nevertheless, they all reach a scale-invariant regime with a steady-state distribution in some of their properties. One would like to understand the evolution and statistical properties of this interesting class of systems, as a simple example of scale-invariant evolution in systems far from thermal equilibrium. Most of the investigations of these systems have concentrated on the two-dimensional (2D) case, which is more accessible to both theoretical and experimental treatments. Experiments on various cellular systems of this type have shown that after a transient period, a scaling regime sets in where all cell statistics reach a steady-state limit up to a uniform rescaling in area. In this regime the area scale, given by the average area of a cell, grows linearly with time, and the distributions of cell-side number and normalized area (the area normalized by the average cell area) become invariant [9–12]. Although the physical processes governing the evolution of these systems are very different from one another, the steady-state distributions are remarkably similar, suggesting a universal mechanism for the creation of such distributions.

These systems were studied in the context of soap foams by Von Neumann [13]. Consider, for example, a 2D array of soap bubbles, made up of liquid film membranes separating gas-filled cells. The gas diffuses slowly across the liquid membranes. If we ignore for a moment the diffusion of the gas, the energy of the system stems from the surface tension of the membranes, and is therefore proportional to the total length of the cell walls. The requirement that this energy be at a local minimum implies that under generic conditions three walls meet at each vertex, and that the angle between walls is 120°. This assures mechanical equilibrium at each vertex. If we now consider the gas diffusion, but assume that the time scale of diffusion is very long relative to the time scale of the wall adjustment, the above conditions at the vertices still hold, but the structure evolves slowly, some cells growing and others shrinking as a result of the diffusion. In this case Von Neumann proved that the growth of each cell is simply given by

$$\frac{da(l)}{dt}=K(l-6)\ , \tag{1.1}$$

$a(l)$ being the area of any l-sided cell (here called an l-cell) and K a constant, depending only on the diffusivity of the gas through the soap film and on the surface tension of the liquid walls. Therefore in such systems all cells with $l<6$ shrink while cells with $l>6$ grow (the total area remaining of course constant). Assuming that three cell sides meet at each vertex, it can be shown from Euler's law ($V-E+F=2$ for the V vertices, E edges, and F faces of a closed two-dimensional graph) that the average number of sides per cell is six in a large system.

In addition to ordinary cell growth, two further processes make up the system's evolution: a neighbor-switching T1 process, and T2 processes where a three-, four-, or five-cell disappears (Fig. 1); T stands for transformation. Such soap foams have been reproduced in experiment [10] and the 120° law and Von Neumann growth law verified.

In other systems analogous mechanisms create a similar evolution of cellular structure. In polycrystals the diffusion between bubbles is replaced by growth of some grains at the expense of others, the curvature of the cell walls resulting from mechanical equilibrium of the grain boundary tensions at the vertices. However, as opposed to the isotropic case of a soap foam, in this case an anisotropy enters the system, since the boundary energy is dependent on the difference in orientation θ between the crystal lattices of the two neighboring domains, and on the orientation of the domain wall. Nevertheless, certain systems have been observed where the effect of the anisotropy is small: most of the cell angles stay close to 120°,

and Von Neumann's growth law is obeyed for most cells. The model for isotropic systems is thus a good first approximation for such polycrystals. For random cellular structures in general, the model allows us to gain insight into the mechanisms driving the evolution of such structures, especially with respect to the existence of a scaling regime and of universality of distributions in such a regime.

Different theoretical approaches have been used for deriving the distributions of two variables of interest that can be measured experimentally, namely, the area and the number of cell sides [14–17]. The models usually take the form of complicated sets of equations, which can only be studied by numerical methods. Recently a model for the distribution of the number of cell sides was introduced [18] where the areas of the cells were integrated out. The resulting dynamical equations for the evolution of the cell-side distribution are simple enough to enable one to get some insight regarding the behavior of the system in the scaling regime. The price one has to pay for this simplicity is the introduction of three phenomenological parameters, to be obtained from experiment. These parameters are the disappearance rates of three-, four-, and five-sided cells. In analyzing the dynamics of these equations it was found that they possess not just a single fixed distribution, but rather a one-parameter family of such distributions. A selection mechanism was proposed according to which a particular fixed distribution is dynamically selected to describe the long-time behavior of the system in the scaling regime.

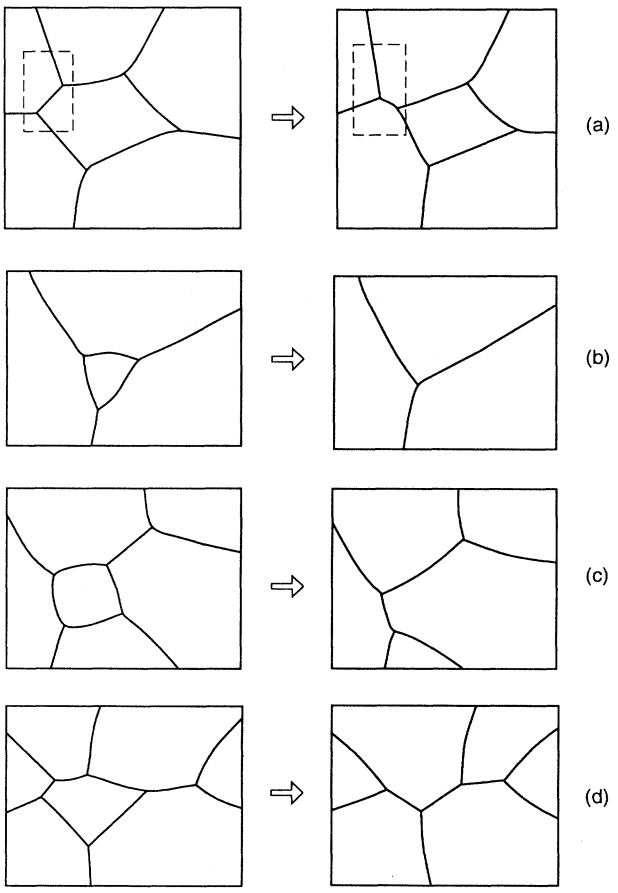

FIG. 1. Processes in cellular systems. (a) shows a T1 process, (b)–(d) three-, four-, and five-cell disappearances.

In this paper we extend the model to include the normalized average areas of l-sided cells, the areas being normalized by the total average area over all cells. The extended model exhibits the same selection mechanism for the fixed-point distribution as the model of Ref. [18]. The model involves four parameters, the three disappearance rates and the Von Neumann growth rate constant K. However, the distributions derived from the model depend only on the ratios between these parameters, so that the predictions of the model are actually dependent on three independent constants. It is found that the average area of l-sided cells grows linearly with l for large l, in accordance with Lewis's law [1]. For small l our results reproduce the deviations from Lewis's law observed in experiments. We also report new experimental results obtained for soap froths, from which the parameters of the model can be determined. Using the experimentally determined parameters, one obtains the average area and the cell-side distributions. Good agreement between these distributions and the experimentally determined ones is found.

The paper is organized as follows. In Sec. II we describe the model for the cell-side distribution and its extension to include the distribution of the average areas. In Sec. III we describe several methods of measuring the parameters of the model and present the experimental results.

II. THE MODEL

We begin by reviewing the model presented in Ref. [18] for the evolution of the number $N_l(t)$ of l-sided cells. We then extend the model to include the average area a_l of these cells, normalized by the area $\bar{a}$ averaged over all the cells in the system.

The statistical properties of the system are described by the variables $N_l(a,t)$, where $N_l(a,t)da$ is the number of l-cells with area between a and $(a+da)$ at a given time. In the scaling regime, reached in the long-time limit, the distributions $N_l(a,t)$ may be written as

$$N_l(a,t)=N_l(a/\bar{a})/t^{\alpha}\ , \tag{2.1}$$

where $\bar{a}$ is the average cell area and α is a scaling exponent. It has been shown [19] that this scaling form together with Von Neumann's law imply that the average cellular area $\bar{a}$ grows linearly in time, and that $\alpha=2$. In our simplified model, we consider the variables

$$N_l(t)=\int N_l(a,t)da\ . \tag{2.2}$$

Since, experimentally, no two-sided cells are found in these systems we take $N_2=0$ as a boundary condition.

As the system evolves, cells with three, four, and five sides shrink at a constant rate by Von Neumann's law. The eventual disappearance of such cells, usually referred to as the T2 processes, change the N_l's, as pictured in Figs. 1(b)–1(d). We denote the disappearance rate of

these cells as w_l ($l=3,4,5$). The disappearance of an l-cell affects not only the number of l-cells, but also the number of sides of the neighbors of the disappearing cell. A three-cell disappearance removes a side from each of its neighboring cells, a four-cell disappearance removes a side from two of its neighbors, and a five-cell disappearance removes a side from two of its neighbors and adds a side to one of its neighbors. Another transformation that affects the N_l is the neighbor-switching or T1 process, pictured in Fig. 1(a). Two of the cells involved in a T1 process lose a side, and the two others gain a side. This process does not change the number of cells. Since experimentally for soap froths T1 processes occur almost exclusively to sides of five-cells, we take them as happening only to such sides, with a rate of w_1.

We now write down master equations for the evolution in the l-cell populations. To describe the change in N_l as a result of an l-cell neighboring a disappearing m-cell, we need to know the probability that a given side of the m-cell belongs to an l-cell. We denote this probability by $P(l,m)$. The equation for the evolution of the population of the three-cells, for example, is then

$$\frac{dN_3}{dt}=-w_3N_3+3w_3P(4,3)N_3+2w_4P(4,4,)N_4 +2w_5P(4,5)N_5+w_1P(4,5)N_5 -w_5P(5,3)N_5-2w_1P(5,3)N_5 . \tag{2.3}$$

The first term represents the disappearance of three-cells, and the next four terms describe four-cells turning into three-cells due to the disappearance of a neighboring three-, four-, or five-sided cell or a T1 process, respectively. The last two terms describe a three-cell turning into a four-cell, due to the disappearance of a neighboring five-cell or a T1 process, respectively.

We now introduce a mean-field approximation for the correlation functions $P(l,m)$. A simple way to do this would be to neglect all correlations and simply write $P(l,m)=lN_l/6N=lx_l/6$, where we denote by x_l the concentration of l-cells, N_l/N. This means taking the probability of a side being an l side as equal to the proportion of l sides among all the $6N$ sides in the system. However, to avoid generating two-sided cells, which do not appear in experimental systems, one has to set $P(3,m)=0$, $m=3,4,5$ for side-removal processes. Setting $P(3,m)$ to zero necessitates adjusting the normalization so that the sum over l of the $P(l,m)$ will remain one. Therefore we take for $m=3$, 4, and 5

$$P(l,m)=\begin{cases}0, & l=3\\ lx_l/(6-3x_3), & l>3 .\end{cases} \tag{2.4}$$

Forbidding three-cell neighbors of a disappearing cell is not necessary for side-addition processes, so there we can simply take the probability for all l as $P(l,m)=lx_l/6$.

Other choices for the $P(l,m)$ are possible, and indeed in the original model of Ref. [18] a slightly different choice was made. However, our equations and those of Ref. [18] give the same general picture for the steady-state solution.

This approximation now gives for the N_3 equation

$$\frac{dN_3}{dt}=-w_3N_3+\frac{4x_4(3w_3N_3+2w_4N_4+2w_5N_5+w_1N_5)}{(6-3x_3)} -3x_3(w_5N_5+2w_1N_5)/6 . \tag{2.5}$$

The equations for the evolution of any N_l can be derived in a similar fashion. If we sum these equations we find

$$\frac{dN}{dt}=-(w_3N_3+w_4N_4-w_5N_5) , \tag{2.6}$$

where as expected, the right-hand side is the total disappearance rate. We now consider the l-cell concentrations $x_l=N_l/N$. Their distribution should not change in the scaling regime, which means that in the scaling regime they should have a distribution which is a fixed point of the evolution equations. These equations for the x_l can be derived from the rates of change of N and N_l. The full equations for the x_l are

$$\frac{dx_l}{dt}=-D_lx_l+K_0x_l+K_1[(l+1)x_{l+1}-\alpha lx_l] -K_2[lx_l-\alpha_l(l-1)x_{l-1}], \quad l=3,4,\ldots , \tag{2.7a}$$

where

$$\alpha_l=\begin{cases}0, & l=3\\ 1, & l>3\end{cases}$$

and the disappearance rates are

$$D_l=\begin{cases}w_3, & l=3\\ w_4+w_1(x_5/x_4) , & l=4\\ w_5-w_l, & l=5\\ 0, & l>5 .\end{cases} \tag{2.7b}$$

Since each T1 process transfers a cell wall that initially borders a five-cell to a neighboring cell, each such process removes one from the five-cell population and adds one to the four-cell population, besides other changes to the general cell population. The disappearance rates are adjusted accordingly for $l=4,5$. The rate constants are

$$K_0=(w_3x_3+w_4x_4+w_5x_5) , \tag{2.7c}$$

the rate of change in the total number of cells,

$$K_1=(3w_3x_3+2w_4x_4+2w_5x_5+w_1x_5)/(6-3x_3) , \tag{2.7d}$$

the cell-side-removal rate coefficient, and

$$K_2=(w_5+2w_1)x_5/6 , \tag{2.7e}$$

the cell-side-addition rate coefficient.

The first term in Eq. (2.7a) describes cell disappearance, the second term comes from the change in the total number of cells, the third term from cell-side removal, and the last term from cell-side addition from five-cell disappearance and T1 processes.

Since T1 processes are observed to be relatively rare, and since calculations show that a slow rate of T1 processes has only a minor effect on the final distributions,

we here neglect these processes and take $w_1=0$.

The equations for the x_l in this case are then

$$\frac{dx_l}{dt}=-w_l x_l+K_0 x_l+K_1[(l+1)x_{l+1}-\alpha_l x_l] -K_2[lx_l-\alpha_l(l-1)x_{l-1}]\ ,\quad l=3,4,\ldots, \tag{2.8a}$$

where $w_l=0$ for $l>5$. The rate constants are now just

$$K_1=(3w_3x_3+2w_4x_4+2w_5x_5)/(6-3x_3) \tag{2.8b}$$

and

$$K_2=w_5x_5/6\ . \tag{2.8c}$$

The equations preserve the two sum rules for the x_l, $\sum_l x_l=1$ and $\sum_l lx_l=6$.

The w_l are the disappearance rates for l-cells, and are free parameters in the mean-field model. Since only the ratios between the w_l determine the fixed distribution, we have two free parameters to determine from experiment. Since the w_l scale the same way in time, $w_l=w_l^*/t$, we will in this section take $(1/t)$ out of the equations as a common factor, and understand w_l^* for w_l.

The evolution equations (2.8) have, as in the equations in Ref. [18], a one-parameter family of steady-state solutions, *for fixed values of the rates* w_l. In the first two equations, only the fixed values of x_3, x_4, and x_5 appear, so given any x_3 satisfying $0\le x_3\le 1$, x_4 and x_5 can be determined by solving these equations. We can then solve iteratively for the rest of the distribution, finding x_l from the $(l-1)$th equation. These equations have the form of a difference equation

$$K_1y_{l+1}-(K_1+K_2)y_l+K_2y_{l-1}+K_0y_l/l=0,\quad l>5\ , \tag{2.9}$$

where $y_l=lx_l$, and K_0, K_1, and K_2 are functions of x_3, x_4, and x_5 [as given in Eq. (2.8)]. This equation has solutions which for large l take the form

$$y_l=\lambda^l l^\kappa\left[1+O\left[\frac{1}{l}\right]\right]\ . \tag{2.10}$$

Inserting this asymptotic form in Eq. (2.9) we find that there exist two solutions of this type with

$$\lambda_1=K_2/K_1,\quad \kappa_1=\gamma$$

and

$$\lambda_2=1,\quad \kappa_1=-\gamma\ ,$$

where $\gamma=K_0/(K_1-K_2)$. Thus for large l the cell-side distribution may be written as a linear combination of the two solutions:

$$x_l\sim A\left[\frac{K_2}{K_1}\right]^l l^{\gamma-1}+Bl^{-\gamma-1}\ , \tag{2.11}$$

where A and B depend on the fixed-point values of x_3, x_4, and x_5, as found from the first two fixed-point equations. On the line of solutions B passes smoothly through zero. The solutions for $B<0$ are unphysical, since they give negative concentrations for large l; the decay at the point $B=0$ is exponential. Linear stability analysis shows that all solutions with $B\ge 0$ are stable.

Since only one fixed point is observed experimentally, Ref. [18] proposed a selection mechanism by which the fixed point corresponding to the distribution with the smallest tail is chosen, i.e., that with the strongest decay for large l. This fixed point is marginally stable. This distribution, which we will call the critical distribution, is closest to all physically reasonable initial distributions, which are necessarily finite, i.e., are such that for some L, $x_l=0$ for all $l>L$. The fixed-point distributions from the Ref. [18] equations all decay exponentially; the critical distribution with the fastest decay is selected. In the model presented in this paper the selected fixed point, that for which $B=0$, is differentiated even more strongly from the other fixed-point distributions, since it is the only one with an exponentially decaying tail. Simulations of distribution evolution from various initial distributions, by integrating Eqs. (2.8), support this selection picture. All finite initial distributions tend to the critical fixed point. The simulations also show that the form of the distribution tail determines the final steady state: in other words, distributions evolve to that fixed point closest to them in its asymptotic (large l) distribution. While all fixed points are stable under a perturbation in the value of a small number of x_l's they evolve to a different fixed point when a global perturbation is made in the distribution of the tail (for example, changing the exponent of decay of x_l with l for all $l>20$), even though the total change made is extremely small.

As a check for the applicability of the mean-field approximation we consider the dynamics of soap froths subjected to T1 processes only. Here we assume that the processes take place in cells with arbitrary number of sides [not just five, as taken in Eq. (2.7)]. For this case the mean-field equations are exactly soluble. Moreover, the exact distribution corresponding to this model has been calculated exactly by Boulatov *et al.* [20] in their studies of fluctuating random surfaces. The mean-field equations for this case are derived in the Appendix. Unlike the model given in Eq. (2.8), where the number of cells decreases with time due to the T2 processes, here the number of cells is conserved and the system reaches a thermodynamic equilibrium. Boulatov *et al.* found that the asymptotic form for large l takes the form

$$x_l\sim(\tfrac{3}{4})^l/\sqrt{l}\ . \tag{2.12}$$

In our mean-field calculation we find that the model exhibits a single stable fixed point (not a line as in the model with T2 processes) with cell-side distribution

$$x_l\sim(0.85)^l/l \tag{2.13}$$

for all l's, in a rather good agreement with the exact result.

We now extend this picture to include as variables the average area of l-cells for the different l's. In the scaling regime the distribution of the average areas a_l for l-sided cells, normalized by the overall average cell area $\bar{a}$, should reach a steady-state limit, as should the distribu-

tion of the total area A_l covered by l-cells. In order to calculate these areas, we do not consider the full distribution $N_l(a,t)$, but rather we write down evolution equations for the a_l (or A_l) again using a mean-field approximation. We note that the average area of l-cells is A_l/N_l, so that the normalized area is given by $a_l = A_l/\bar{a}N_l$. Using $\bar{a} = A/N$, where A is the total area, and $N_l = Nx_l$, we have $a_l = A_l/Ax_l$. The central assumption that allows us to directly write a model for the a_l is that when an l-cell turns into an $(l\pm1)$-cell, as a result of the disappearance of a neighboring cell, it does so with the average l-cell area, a_l. The resulting equations allow a simple treatment of area averages without using a full model for the joint distributions of area and cell-side number. The price of this simplification, as we will see, is the addition of a new free parameter, not determined by the theory, namely, the cell growth constant as appearing in Von Neumann's equation (or rather, the ratio between Von Neumann's constant and the disappearance rates). In a full microscopic model the fixed-point distribution would not be dependent on any free parameters, the disappearance rates being derivable from Von Neumann's constant and the density of cells at zero area.

To illustrate the structure of the equations for the areas we consider the rate of change in the total area covered by three-cells A_3. This rate of change, $\partial A_3/\partial t$, is made up of three contributions: the usual Von Neumann growth rate $-3KN_3$, the addition of area from four-cells at an average area of A_4/N_4 joining the three-cell population at a rate of $4N_4K_1$, giving a contribution of $4N_4K_1(A_4/N_4)$, and the decrease of area from three-cells turning into four-cells, $3N_3N_3K_2(A_3/N_3)$. Thus the equation for the evolution of the total three-cell area is

$$\frac{\partial A_3}{\partial t} = -3KN_3 - 3K_2A_3 + 4K_1A_4 \ . \tag{2.14}$$

The general equation for the evolution of l-cells is derived in much the same way:

$$\frac{\partial A_l}{\partial t} = (l-6)KN_l + K_1[(l+1)A_{l+1} - \alpha_l l A_l] + K_2[\alpha_l(l-1)A_{l-1} - lA_l] \ , \tag{2.15}$$

where α_l is defined in Eq. (2.7). The equations for the normalized average cell areas a_l are then easily derived from the relation $a_l = A_l/Ax_l$, so that

$$\frac{\partial a_l}{\partial t} = (1/Ax_l)\frac{\partial A_l}{\partial t} - (A_l/Ax_l^2)\frac{\partial x_l}{\partial t} \ . \tag{2.16}$$

Substituting Eqs. (2.8) and (2.15) we have

$$\frac{\partial a_l}{\partial t} = K'(l-6) + w_l a_l - a_l K_0 + K_1\frac{(l+1)x_{l+1}}{x_l}(a_{l+1}-a_l) + \alpha_l K_2\frac{(l-1)x_{l-1}}{x_l}(a_{l-1}-a_l) \ , \tag{2.17}$$

where $K' = K/\bar{a}$. Since $w_l \sim (1/t)$ and $\bar{a} \sim t$, all terms scale the same way with time and we again implicitly factor t out of the equation. The first term represents the regular Von Neumann growth, the second term represents the change due to three-, four-, and five-cell disappearance with zero area, the third term the change in the average area due to the change in the total number of cells, the fourth term the change due to an $(l+1)$-cell with area a_{l+1} joining the l-cells with area a_l, and the last term the change due to an $(l-1)$-cell with area a_{l-1} turning into an l-cell. Note that when an l-cell turns into an $(l\pm1)$-cell, the average area of the l-cells does not change, since it is assumed that the area of the disappearing l-cell is equal to the average area a_l.

The extended model thus consists of two sets of equations: one set [Eq. (2.8)] for the rate of change in the x_l involving the x_l only, the other set [Eq. (2.17)] for the rate of change in the a_l involving both the a_l and the x_l. To find the fixed point we solve the first set for the x_l, find the fixed point chosen by the selection mechanism, then solve the second set of equations for the a_l with the x_l acting as parameters [21].

The a_l fixed-point equations have a one-parameter family of solutions. However, only one of these solutions obeys the sum rule

$$\sum_{l=3}^{\infty} x_l a_l = 1 \ , \tag{2.18}$$

which should be satisfied by the definition of the normalized a_l.

While experimentally the normalized average area of the three-cells is of order of magnitude 10^{-2}, this is by no means the case for the solutions obeying the sum rule for all given K, w_3, w_4, and w_5. For given w_l, a_3 has a strong linear dependence on K, and only for a very narrow range of K's do we get a reasonable answer for a_3. Thus a given set of w_l's effectively determine K. For the set of experimentally determined w_l (see Sec. III) we find that K' must be equal to 1.0.

The dependence of a_l on l for the physically reasonable solutions (those with small a_3) becomes close to linear for $l > 6,7$ (see Fig. 2). The a_l equation for $l \to \infty$ gives, for the asymptotic slope γ (so that $a_l \sim \gamma l$),

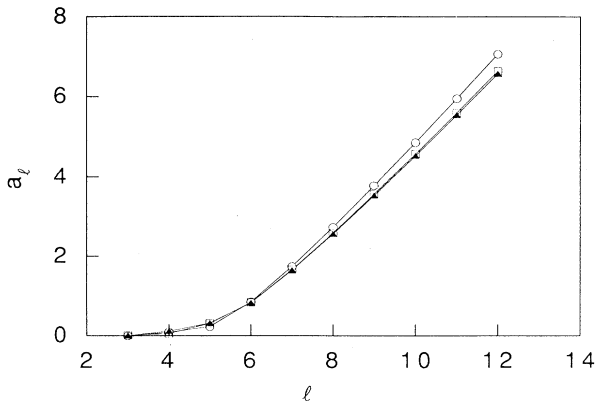

FIG. 2. Theoretical area distribution for various sets of rate coefficients. The triangles denote $w_l = \{24,6,1\}$, squares denote $w_l = \{48,6,1\}$, and the circles denote $w_l = \{36,10,1\}$. The lines serve as guides to the eye.

$$\gamma=\frac{K'}{K_0+K_1-K_2} . \tag{2.19}$$

Furthermore, it is easy to show that if we assume an asymptotic power-law dependence of a_l on l then the only solution is linear in l. Lewis conjectured on the basis of experimental observations that a_l is linear in l (Lewis's law). The conclusion from our model is that this law is satisfied only asymptotically. Since the w_l essentially determine the K, they also determine the slope γ, which turns out to have quite a weak dependence on the w_l chosen (Fig. 2).

III. EXPERIMENTAL METHODS AND RESULTS

In order to compare the predictions of the model described in the preceding section with experimental distributions, one has to determine the values of the time-independent ratios w_3/w_5, w_4/w_5, and K'/w_5 from experiment. One may then use them as input parameters to calculate the cell-side and area distributions in the model. It has been found from experiments that triangular cells appear so rarely that it is impossible to determine their rate of disappearance w_3. Therefore in our experimental observations we refer only to cells with four or more sides, and compare the results to a model in which three-sided cells do not appear. Such a model is trivially constructed in the same way as the model presented in the previous sections. The creation of three-cells is prevented in the same way that the creation of two-cells is prevented in the usual model. In this section we describe three independent methods we used to determine these parameters from experiments on soap froths, and present our results. The experimental system itself has already been described in Ref. [10], to which we refer the reader for details.

Perhaps the best way of extracting the values of w_4/w_5 and w_5/K' from experimental data has been described in Ref. [18]. It is based on the relationship between the rates of disappearance w_l and the quantities $N_l(0,t)$,

$$w_l=K(6-l)N_l(0,t)/N_l(t) . \tag{3.1}$$

One can therefore find the ratios of the w_l by finding the ratio between the respective zero-area densities $\rho_l=N_l(0,t)/N_l(t)$ at any given time. Note that these densities scale like $1/t$. The easiest way to implement this method is to plot the total number $M_l(a)$ of l-cells having an area up to a given value a as a function of a. The slope of this plot at the origin is ρ_l and thus from Eq. (3.1) one obtains the ratio

$$w_4/w_5=2\rho_4/\rho_5 . \tag{3.2}$$

We show in Fig. 3 typical plots for $M_4(a)$ and $M_5(a)$. The values of ρ_l extracted from these plots yield

$$w_4/w_5=7.6\pm0.5 . \tag{3.3}$$

Further use of Eq. (3.1) and the definition of K' yield

$$w_5/K'=\bar{a}(t)\rho_5 . \tag{3.4}$$

In using this equation, $\bar{a}(t)$ is measured for the same time

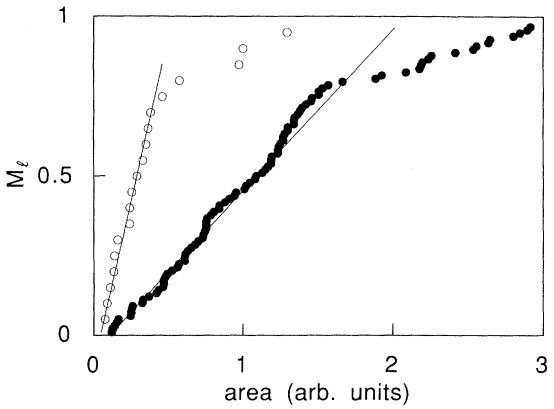

FIG. 3. Number of four- and five-sided cells having area up to a given a, taken from experiment. The disappearance rates can be found from the slope at zero. Empty circles represent five-sided cells, full circles four-sided cells. The area is in arbitrary units, and the lines serve as a guide to the eye.

t as the density ρ_5. A typical plot of $\bar{a}(t)$ is shown in Fig. 4. These measurements yield

$$w_5/K'=1.70\pm0.20 . \tag{3.5}$$

A direct way of measuring w_4/w_5 is based on the definition of the parameters w_l:

$$w_l=\frac{1}{N_l}\left[\frac{dN_l}{dt}\right]_{\rm dis}=\frac{1}{N_l}\frac{\Delta N_l^{\rm dis}}{\Delta t} , \tag{3.6}$$

where $\Delta N_l^{\rm dis}$ is the number of l-cells that disappear during a time interval Δt. $\Delta N_l^{\rm dis}$ accounts for the actual disappearance of l-cells, and not for their elimination due to neighbor disappearances. Thus w_l can be estimated by measuring $\Delta N_l^{\rm dis}$ from consecutive pictures taken at short-time intervals. Using this method we obtained

$$w_4/w_5=6.6\pm0.7 , \tag{3.7}$$

which is consistent with the value obtained with the previous method.

Finally, a third method enabled us to determine the

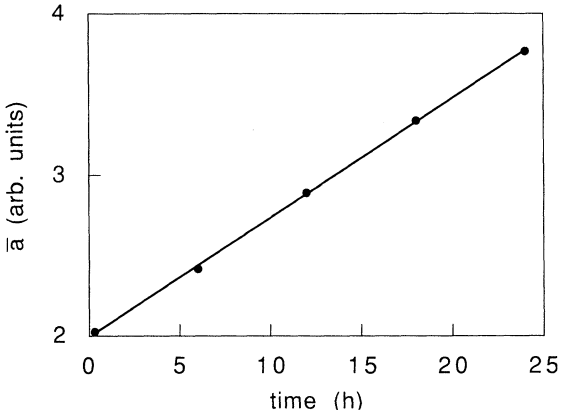

FIG. 4. A typical experimental plot of average cell area as a function of time.

value of w_5/K' from the same sequence of pictures by measuring w_5 and K' separately. To measure w_5 we used the scaling assumption, according to which N_l must scale as $1/t$ in order for the x_l to be time independent. One can then define the time-independent quantity N_l^* by

$$N_l = N_l^*/t \ . \tag{3.8}$$

Using Eq. (3.1) and the time-independent quantities w_l^* defined in Sec. II we obtain

$$\left[\frac{dN_l}{dt}\right]_{\text{dis}} = \frac{w_l^* N_l^*}{t^2} \tag{3.9}$$

while differentiating Eq. (3.8) yields

$$\frac{dN_l}{dt} = -\frac{N_l^*}{t^2} \ . \tag{3.10}$$

Dividing the latter two equations one by the other we obtain

$$\left[\frac{dN_l}{dt}\right]_{\text{dis}} = -w_l^* \frac{dN_l}{dt} \ , \tag{3.11}$$

which when integrated yields

$$N_l^{\text{dis}}(t) = -w_l^* N_l(t) + c \ . \tag{3.12}$$

Here $N_l^{\text{dis}}(t)$ is the total number of l-cells which have disappeared up to time t. Thus a simple count of cell disappearances over a given time period yields w_5^*. In Fig. 5 we show a plot of $N_l^{\text{dis}}(t)$ as a function of $N_l(t)$, whose slope yields w_5^*. We obtained $w_5^* = 2.1 \pm 0.1$ from which w_5 can be obtained by multiplying t. K' can be extracted from the data from direct measurements of Von Neumann's constant K and the average area $\bar{a}$. This yields

$$w_5/K' = 1.7 \pm 0.2 \ , \tag{3.13}$$

in agreement with the values obtained with the previous method.

This value is different from the theoretical one, $w_5/K' = 1.0$ (see Sec. II). We have seen that our simple model assumes that l-cells losing sides by the disappearance of neighboring cells have the average l-cell area a_l. Experimental observations indicate, however, that it is more accurate to assume that l-cells losing sides have an area equal to the average of a_1 and a_{l-1}. This is easily incorporated into the model, and the results indeed give a value for K' consistent with the experimental value. The other predictions of the model are not affected significantly by this change.

The results of our measurements of the x_l and a_l distributions are shown in Figs. 6 and 7. The agreement with our model's prediction is very good in the case of the x_l, while in the case of the a_l the theory successfully predicts the qualitative behavior of the experimental distribution, with some numerical discrepancy for some values of l. The experimental results bear out our theoretical prediction that Lewis's law of linear dependence is satisfied only asymptotically.

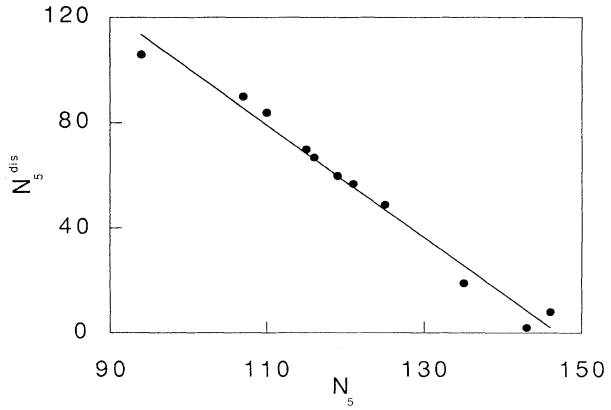

FIG. 5. The number of five-sided cells that have disappeared by shrinking up to a given time, N_{dis}, vs the number of five-cells at that time.

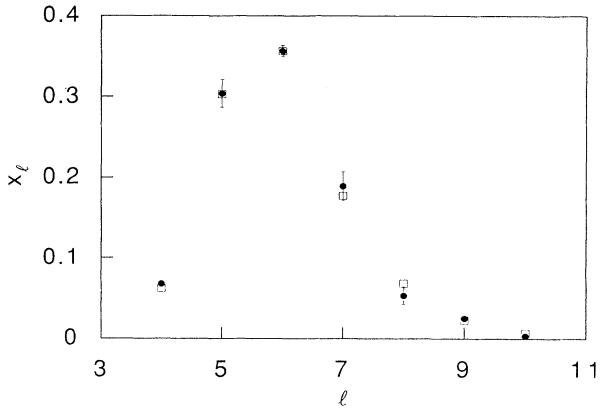

FIG. 6. Experimental and theoretical results for x_l. The squares represent the theoretical results, with the parameters taking their experimental values ($w_4/w_5 = 7.6$), and the circles with error bars represent the experimental values.

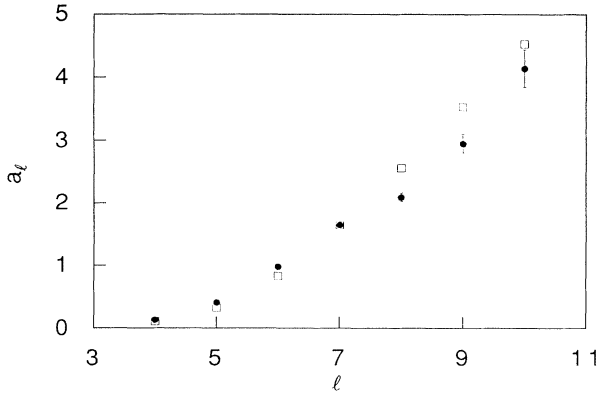

FIG. 7. Experimental and theoretical results for a_l. The squares represent the theoretical results, for the same parameters as in Fig. 6 and the circles with error bars represent the experimental values.

IV. SUMMARY AND CONCLUSIONS

We have presented an extension of previous work, on the distribution of cell sides x_l in a random cellular system, to the distribution of the average areas of l-cells a_l. The extended model uses the same selection mechanism used in the original model to arrive at a single universal distribution, but adds to the model an additional free parameter, the Von Neumann growth constant. Actually, as we see, physical constraints on possible area distributions practically determine this parameter, within a narrow range. The derived area distribution is compared to distribution measurements in soap froths, and good qualitative agreement is shown. Lewis's law (linear dependence of average area on cell-side number) is confirmed asymptotically, both theoretically and experimentally. Finally, we remark that it would be interesting to consider a model for the detailed area distributions $N_l(a,t)$, particularly with respect to the size of the space of fixed points and selection mechanisms.

ACKNOWLEDGMENTS

We thank E. Domany and A. Jacobs for fruitful discussions. This work was supported in part by grants from the Israel-U.S. Binational Science Foundation (BSF), Jerusalem, Israel. J. S. acknowledges support from the Revson and Minerva Foundations.

APPENDIX A: A DUALITY BETWEEN SURFACE TRIANGULATIONS AND CELLULAR STRUCTURES

In studies of fluctuating random surfaces, the geometry of the plane is approximated by a triangulation, a tiling of the plane by triangles. The curvature of the surface at each vertex is related to the number of triangles meeting at that vertex. The triangulations of the plane are counted by looking at the dual lattice, which is a cellular structure with three walls meeting at each vertex. Counting over all such graphs is performed by permuting a given graph by manipulations formally identical to what is described above as the T1 process (see Fig. 1). Since a dynamics of T1 processes is ergodic [20], the statistics of such graphs should correspond to the fixed-point distributions of a dynamic model which includes only T1 processes. To model this process using our approach, we define a rate constant W for the T1 process, the probability of a T1 process in unit time per line. Each such event results in the removal of a side from two cells and the addition of a side of two others. The process cannot take place if either of the cells initially sharing the side is a three-cell, so as to ensure that two-cells are not created. The dynamic equations for the x_l are then

$$\frac{dx_l}{dt} = W\left[1-\frac{x_3}{2}\right][(l+1)x_{l+1}-lx_l] + W\left[1-\frac{x_3}{2}\right]^2[(l-1)x_{l-1}-lx_l] \tag{A1}$$

for $l>3$. This model possesses a single fixed-point distribution which

$$x_l \sim \lambda^l/l \ , \tag{A2}$$

where $\lambda \approx 0.85$. On the other hand, the exact random surfaces calculations give for the same distribution the asymptotic result

$$x_l \sim \lambda^l/\sqrt{l} \ , \tag{A3}$$

with $\lambda = \frac{3}{4}$. We see that the qualitative form of the solution is quite similar.

[1] D. Weaire and N. Rivier, Contemp. Phys. **25**, 59 (1984); N. Rivier, Philos. Mag. B **52**, 795 (1985).
[2] R. W. Armstrong, Adv. Mater. Res. **4**, 101 (1970).
[3] C. J. Simpson, C. J. Beingessner, and W. C. Winegard, Trans. Metall. Soc. AIME **239**, 587 (1967).
[4] S. K. Kurtz and F. M. A. Carpay, J. Appl. Phys. **51**, 5725 (1981).
[5] K. L. Babcock and R. M. Westervelt, Phys. Rev. A **40**, 2022 (1989).
[6] K. L. Babcock and R. M. Westervelt, Phys. Rev. Lett. **64**, 2168 (1990).
[7] K. L. Babcock, R. Seshardri, and R. M. Westervelt, Phys. Rev. A **41**, 1952 (1990).
[8] D. Weaire, F. Bolton, P. Molho, and J. A. Glazier, J. Phys. Condens. Matter **3**, 2101 (1991).
[9] J. A. Glazier, S. P. Gross, and J. Stavans, Phys. Rev. A **36**, 306 (1987); J. Stavans and J. A. Glazier, Phys. Rev. Lett. **62**, 1318 (1989).
[10] J. Stavans, Phys. Rev. A **42**, 5049 (1990).
[11] B. Berge, A. Simon, and A. Libchaber, Phys. Rev. A **41**, 6893 (1990).
[12] K. J. Stine, S. A. Rauseo, B. G. Moore, J. A. Wise, and C. M. Knobler, Phys. Rev. A **36**, 306 (1987).
[13] J. Von Neumann, in *Metal Interfaces,* edited by C. Herring (American Society of Metals, Cleveland, 1952), p. 108.
[14] M. P. Marder, Phys. Rev. A **36**, 438 (1987).
[15] J. R. Iglesias and R. M. C. de Almeida, Phys. Rev. A **43**, 2763 (1991).
[16] V. E. Fradkov, D. G. Udler, and R. E. Kris, Philos. Mag. Lett. **58**, 277 (1988).
[17] C. Beenakker, Physica A **147**, 256 (1987).
[18] J. Stavans, E. Domany, and D. Mukamel, Europhys. Lett. **15**, 479 (1991).
[19] W. W. Mullins, J. Appl. Phys. **59**, 1341 (1986); Scr. Metall. **22**, 1441 (1988).
[20] D. V. Boulatov, V. A. Kazakov, I. K. Kostov, and A. A. Migdal, Nucl. Phys. **B275**, 641 (1986).
[21] In principle, similar equations may be derived from the equations for the evolution of the joint distribution of area and cell-side number $\rho(a,l)$. H. Flyvbjerg and C. Jeppesen [Phys. Scr. **T38**, 49 (1991)] have derived such a set of equations which can be shown to be consistent with ours except for some small differences (e.g., their model includes zero-, one-, and two-sided cells).